Progress In Electromagnetics Research M, Vol. 113, 199–211, 2022

Compact Embedded Dual Band EBG Structure with Low SAR for Wearable Antenna Application

Vidya R. Keshwani[1, *], Pramod P. Bhavarthe[2], and Surendra S. Rathod[3]

Abstract—In this paper, a rectangular embedded dual band Electromagnetic Band Gap (EBG) structure at frequencies 2.45/5.8 GHz useful in industrial, scientific, and medical (ISM) band for various wearable applications is proposed. The main intent of this work is to design a dual-band EBG to reduce specific absorption rate (SAR). The unit cell which is a part of the EBG structure is formed using a rectangular patch. It has a U-shaped rectangular slot and a stretched strip with a rectangular patch at end. EBG unit cell simulation is accomplished by solving eigen-mode problem in High Frequency Structure Simulator (HFSS). EBG structure has to be suitably designed and fine tuned for specified band stop property to reduce surface waves. It must improve front to back ratio (FBR). With placing antenna on human body, frequency detuning occurs which is undesirable thus emphasizing the need of improvement in impedance bandwidth. This improvement can be achieved by a suitable design of EBG structure. In this work, the proposed EBG structure is integrated with a dual-band monopole antenna at frequencies 2.45/5.8 GHz for wearable application. The evaluation of antenna performance on a four layer body model is carried out. Simulations are used to demonstrate EBG array structure effectiveness for the reduction of Specific Absorption Rate (SAR) on the four layer body model. Computed SAR values for tissue in 1 g and 10 g are within standard prescribed limits. It is concluded that the proposed dual-band antenna is appropriate for wearable applications. Proposed EBG array is fabricated and integrated with a twin E-shaped monopole antenna. The measurement of reflection coefficient, radiation pattern, and transmission coefficient of fabricated EBG array is carried out. The measured and simulated results show good agreement. Antenna performance in the event of bending condition and on-body condition is assessed.

1. INTRODUCTION

In recent past, flexible wireless devices have been found quite increasingly for advanced communication systems in various applications. Some of related modern applications include Internet of Things (IoT) and 5G technology. These wearable devices help not only monitor and record many physiological parameters of the human body but also transmit the essential information with minimum power consumption [1]. Wireless body area network (WBAN) may be classified into single-sensor link (SSL) and multi-sensor link (MSL). Multiple sensor nodes make use of MSL network. They are distributed at different locations in human body and work in synchronous manner. Multiband antennas with flexibility and compactness are an important part of such systems [2]. Dual and multifrequency antennas are often needed for wireless products having multi-functionality. It reduces the component count and subsequently hardware size [3]. Wearable industry demands the antenna that exhibits high gain and

Received 17 July 2022, Accepted 7 September 2022, Scheduled 22 September 2022

* Corresponding author: Vidya R. Keshwani (vrkeshwani@gmail.com).

[1] Department of Electronics Engineering, Sardar Patel Institute of Technology, Andheri(w), Mumbai 400058, India. [2] Department of Artificial Intelligence and Data Science, Vasantdada Patil Pratishthan's College of Engineering and Visual Arts, Sion, Mumbai 400022, India. [3] Department of Electronics & Computer Engineering, Fr. Conceicao Rodrigues College of Engineering, Bandra, Mumbai 400050, India.

efficiency, low SAR, and at the same time it must be flexible [4]. For achieving the feature of flexibility as well as comfortability, researchers usually fix antenna on materials. Such materials are classified as flexible materials. Most preferred materials in this case are textile materials. They offer advantages such as ease of integration with clothes. For applications in wearable antenna devices, textile materials used most are felt, leather, denim, silk, etc. They offer unmatchable comfort and skin friendliness. Nevertheless, most importantly antenna designer must aim for the lowest possible SAR. It is a quite important parameter for the determination of safety levels of wearable antennas. SAR should be less than acceptable limit imposed by standards. Organizations namely IEEE, ICNIRP, FCC have imposed limits on amount of radiation emission from these devices. This is emphasized with intent of public protection from overexposure to EM fields. Guidelines by FCC and ICNIRP impose that SAR must be less than 2 W/kg averaged over 10 g of human tissue. Also it must be less than 1.6 W/kg averaged over 1 g [5–7].

In past variety of techniques have been proposed by various authors in literature to minimize SAR. Here mainly two approaches are mentioned. (1) SAR reduction can be achieved by using an antenna with suitable size ground plane. Ground plane shall act as a shield for human body, thus minimizing radiation transmitted to human body. However, textile antennas of large size with a full ground plane are highly sensitive to deformation. (2) Incorporation of artificial magnetic conductors (AMC), referred to as EBG structure and high impedance surfaces. EBG is used as a backing shield for wearable antenna. This leads to the minimization of surface waves thus lowering radiation toward the human body surface and subsequently antenna exhibiting improvement in overall gain and FBR [4].

AMC/EBG based wearable antenna designs lead to large size, which limits their application in cases where there is space constraint [1]. However in recent past, variety of EBG structures have been investigated and published for single and dual-band frequencies. EBG has the ability of prevention of propagation of EM wave in specified direction or frequency. In the band gap regime, due to high surface impedance property, they exhibit radiation performance enhancement in terms of gain and also due to reduction in side lobes. This makes them a preferred candidate for wearable antenna applications where reduced or minimum SAR is the main requirement. In wearable applications, it is generally desirable to use a uniplanar, compact, EBG structure with no vias as vias affect comfortness [8].

In past various authors have reported various types of single/dual band EBG structures. In [9], a double concentric square dual-band EBG comprising EBG unit cell of patch size of $0.327\lambda_{c1}$, operating at 2.45 GHz and 5 GHz (λ_{c1} is the operating frequency of antenna) is reported. Radiations penetrating into body are reduced as investigated. Authors in [10] report a dual-band antenna integrated with EBG at 2.4/5 GHz having dimensions of $100 \times 100 \times 4.5\,\text{mm}^3$ and unit cell array of 4×4. A textile antenna with high FBR and low SAR value in a wide band is investigated. It uses a substrate made up of felt material with 1.5 mm thickness. In [11], the authors report a metamaterial based dual-band antenna using textile as a substrate with size in mm^3 as $50 \times 50 \times 6.35$ and unit cells 2×2. It works at frequencies of 2.4/5.2 GHz. The substrate is made up of felt material of 6 mm thickness. In [12], the authors report a coplanar waveguide antenna of dual-band type, over an AMC structure which operates at 2.4/5.8 GHz. The AMC used is a 3×3 array with a periodicity of 40 mm. The overall antenna dimensions are $109 \times 120 \times 3.2$ mm. In [13], the authors report a 3×3 rectangular ring shape array and its equivalent circuit model of EBG. The designed unit cell has size $0.216\lambda_{c1}$ of dimensions 81 mm × 81 mm.

In this paper, the authors attempt to design a compact PDEBG structure as compared to other reported EBG structures [9, 14–18]. This type of structure offers lot of advantages compared to other reported structures for wearable antennas. Asymmetric/anisotropic unit cell when being used as EBG exhibits polarization dependence (PD). For PDEBG the surface wave band gap and reflection phase band gap may differ from each other in different orthogonal directions. Compact EBG microstrip line has been designed by authors in [19] using surface wave band gap property of PDEBG. In our work, structure compactness is attained by using a novel U-shaped slot, stretched strip, and rectangular slot embedded in adjacent PDEBG without vias. The authors propose a purely textile antenna with low profile. Multiband characteristic is achieved using a PDEBG structure. Also, good isolation is attained with low SAR level. The proposed antenna covers the ISM band.

Section 2 presents the design of proposed EBG unit cell, EBG array, and its related simulation results. The comparison of simulated and measured EBG characteristics using SML method is carried

out. In Section 3, E-shaped monopole antenna, its simulated radiation pattern, and reflection coefficient are described. Simulation results of antenna integrated with the proposed EBG array S_{11} along with parametric studies are described. The comparison of simulated and measured reflection coefficients and radiation patterns of antenna integrated with EBG is also mentioned. The effect of antenna bending on S_{11} is bought out using measured results. In Section 4, SAR analysis by simulation studies using the proposed EBG structure on a 4-layer body model is elaborated. It also brings out the comparative assessment of proposed EBG structure with reported structures at 2.45 GHz and 5.8 GHz followed by conclusions in Section 5.

2. PROPOSED EBG DESIGN AND SIMULATION RESULTS

The common approach to implement an EBG structure is to use periodic arrangement of conductors and dielectric materials. Periodic repetition along x and y axes has contribution to properties of band gap and band stop. Reflection phase diagram and lumped circuit model are useful to extract band stop property [20]. Ansys HFSS simulation software has been used for the modeling of EBG structure. This software is useful for carrying out different types of simulations of various types of antenna structures with various properties. Important insights are obtained from these simulations by obtaining reflection phase plot for a given dimensions of EBG unit cell, reflection coefficient for antenna, its radiation pattern, etc.

2.1. Proposed EBG Unit Cell and Its Simulation Results

Each unit cell of the proposed EBG has a rectangular patch with a rectangular slot which is U-shaped. It has a stretched strip with rectangular patch at its end and embedded in adjacent EBG. The rectangular patch is formed with a rectangle of appropriate dimension and encompasses another square patch located at the center. Additional capacitance is obtained due to the gap between the square slot & the inner patch embedded in the adjacent EBG cell. Dimensions of EBG unit cell and its inner parts are shown in Figure 1. In Figure 1, all dimensions are in mm. Here, $x = 40$, $a = 5.25$, $b = 13.5$, $c = 10$, $d = 10$, $e = 0.5$, $f = 4$, $i = l = 2$, $j = 3$, $k = 1$, $h = 2$, $g = 2.5$. These dimensions can be further referred by below terminology pertaining to EBG structure and its properties. The width and height of substrate $(x) = 40$; substrate dielectric constant $(\epsilon) = 1.7$; substrate thickness = 1; copper thickness $(t) = 0.17$; rectangular patch width $(2a+b)$ is 24; its height $(c+d)$ is 20; width of the U-shape slot (b) is 13.5; height

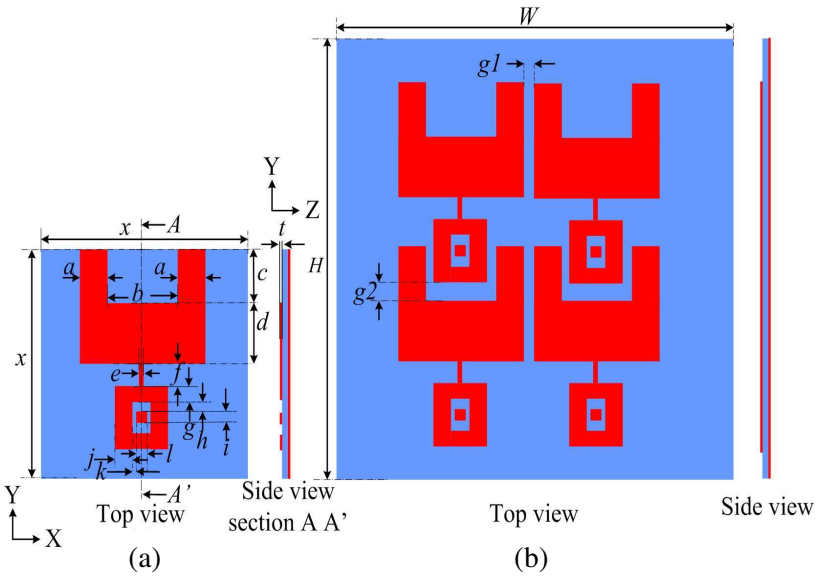

Figure 1. (a) EBG unit cell. (b) EBG array.

of the U-shape slot (c) is 10; width of the stretched strip (e) = 1; the height of the stretched strip is 4; patch located at the end of stretched strip has width ($2j + 2k + l$) = 10 and height ($2g + 2h + i$) = 11; width of outer slot (j) = 3.00; outer slot height (g) = 2.5; inner patch width (l) = 2.00; inner patch height (i) = 2.00. Above selected dimensions helped to achieve the dual band resonance frequencies $f1 = 2.45$ GHz and $f2 = 5.8$ GHz. By adjusting the i (height of the inner patch) and width of patch located at the end of stretched strip ($2j + 2k + l$), different values of cutoff frequencies can be obtained around $f1$. Cutoff frequencies around $f2$ can be changed by varying dimension a. Lot of microwave applications need this feature of band gap centre frequency variation.

2.2. Simulated Reflection Phase

The analysis of EBG structure in both X and Y polarizations can be carried out by two master/slave boundaries on the sides of EBG unit cell. By deembedding the impedance of wave port up to the top of cell, the phase of the reflection coefficient is obtained. Figure 2 shows the plot of simulated reflection phase with a plane wave normally illuminating the PDEBG surface. It is seen that the designed EBG structure reflects normal incident wave with a zero degree phase at frequencies 2.64 GHz and 6.16 GHz in X polarization and Y polarization at 2.10 GHz and 5.8 GHz.

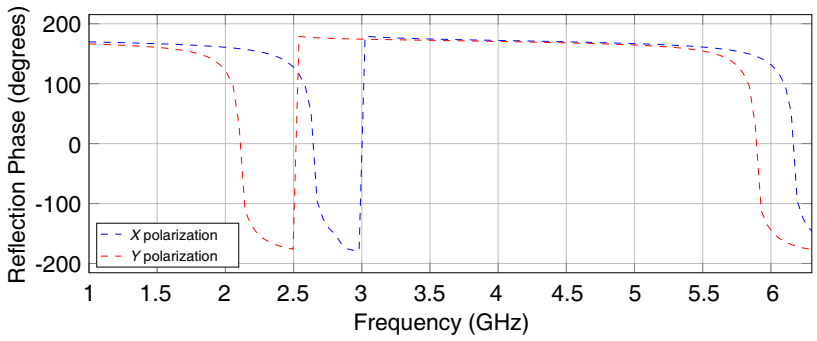

Figure 2. Plot of simulated reflection phase of proposed dual band EBG unit cell.

2.3. EBG Array, Its Simulation and Measured Results

A 2 × 2 EBG array is obtained from EBG unit cells (Figure 1). Here all dimensions are in mm. Dimensions are substrate width (W) = 63 and its height (H) = 75, inter-gap between two EBG unit cells ($g1$) = 1. $g2 = 2$ is a gap between outer slot at the end of stretched strip and embedded in U-shape slot of adjacent EBG & inner square patch. It was observed during simulations that as distance between square patch located at the end of stretched strip & slot strip of the adjacent PDEBG (in EBG array) is reduced, higher value of capacitance can be obtained.

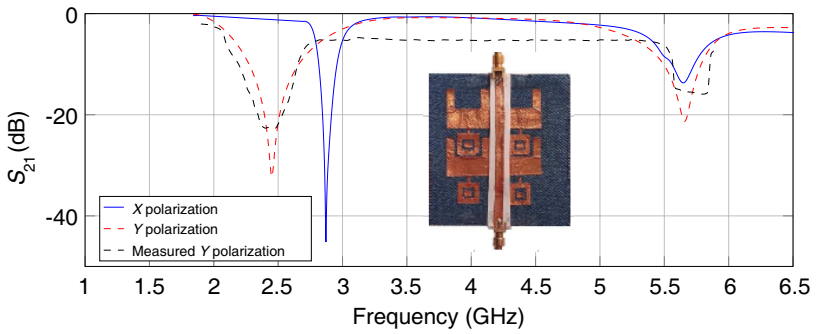

Figure 3. Comparison of simulated and measured EBG characteristics (S_{21}) using SML method.

For verification of the band stop property of the PDEBG, 2×2 cells are simulated by suspended microstrip line (SML) method. In SML method, microstrip line is kept at the distance of 0.2 from EBG surface in simulations. Simulation results reveal (Figure 3) band gap with a center frequency of 2.89 GHz and 5.61 GHz in the x direction. A band gap is obtained with a center frequency 2.76 GHz with 5.63 GHz in the y-direction. Here, a frequency range exhibiting attenuation loss less than -10 dB is considered as the band gap [21]. Figure 3 also shows the comparison of simulated and measured results in y-direction along with fabricated EBG array with SML. As per measured S_{21} in y-direction center frequencies are 2.42 GHz and 5.7 GHz.

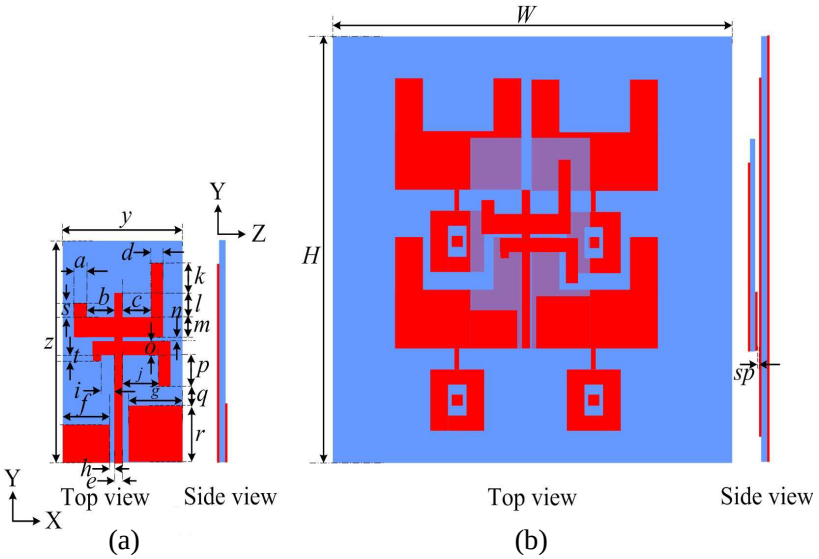

Figure 4. (a) Twin E-shape monopole antenna. (b) Monopole antenna with EBG.

3. PERFORMANCE OF PROPOSED EBG WITH MONOPOLE ANTENNA

3.1. Twin Rotated E-Shaped Monopole Antenna Design

The dual-band antenna considered in this work is a monopole antenna which is fed by a coplanar waveguide (CPW) and has an asymmetry in ground plane (shown in Figure 4(a)). The dual-band antenna consists of twin rotated E-shaped monopoles. They are connected to the end of the CPW transmission line. All dimensions in Figure 4 are in mm. Here, $a = 2$, $b = 4.7$, $c = 4.9$, $d = 2$, $s = 2$, $l = 5$, $m = 3$, $k = 1$, $n = 1$, $t = 1$, $o = 2$, $p = 3$, $q = 5$, $g = r = 9$, $f = 8$, $h = 0.8$, $e = 1.4$, $i = 2.5$, $j = 5.8$, $y = 20$ and $Z = 35$. The proposed antenna is designed on denim material as a substrate having thickness 0.7. Denim material has dielectric constant $\epsilon_r = 1.7$ and tangent loss = 0.02. The copper tape thickness is 0.017. The feed line for the antenna is made up by the use of a CPW transmission line comprising a strip width (e) of 1.4 and length ($p + q + r + o$) as 20. The strip is separated from ground by the gap (h) of 0.8 mm. The design steps of dual-band antenna for ISM band applications comprise properly selecting the dimensions of twin E shapes and those of partial ground plane numerically.

Simulated radiation patterns of above antenna in Y-Z plane, i.e., in E-plane, & X-Z plane, i.e., in H-plane, at frequencies 2.45 GHz and 5.8 GHz are shown in Figure 5. It is observed that at both frequencies, antenna shows an omnidirectional pattern in H plane and a bidirectional pattern in E plane.

3.2. Antenna Integrated with EBG

The antenna integrated with proposed EBG array is as shown in Figure 4(b). The spacing between antenna and EBG array (sp) is 1 mm. Figure 8 shows the simulated refection coefficient S_{11} of designed

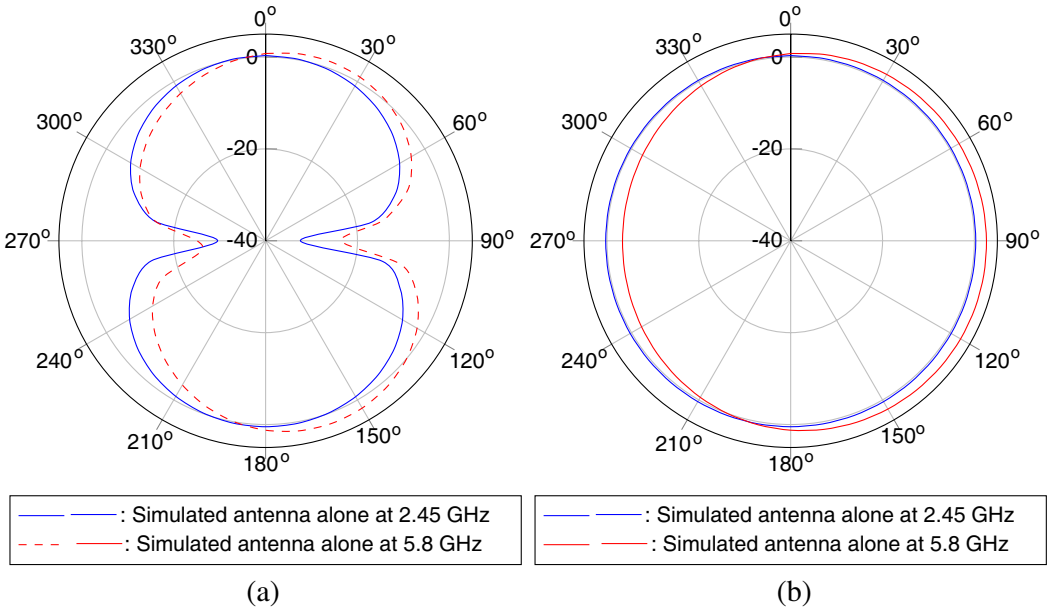

Figure 5. Simulated radiation patterns of antenna without EBG in (a) E plane and (b) H plane.

antenna in free space. Without EBG, only antenna shows that S_{11} at frequency of 2.457 GHz is -16.7385 dB and at frequency of 5.8175 GHz is -17.7654 dB.

Figure 4(a) shows dimensions of antenna which are selected so as to resonate with EBG in dimensions shown in Figure 2. EBG dimensions j and a were varied (keeping all other parameters constant) to carry out parametric study on S_{11} of EBG integrated with antenna. Table 1 shows the effect of j and a on S_{11}. In above study, j values of 2.5, 3, and 4 were considered keeping $a = 5.25$. Minimum S_{11} at both frequencies $f1$ and $f2$ was observed for $j = 3$ and $a = 5.25$. Further, keeping $j = 3$, values of a were changed to 4.75, 5.25, and 5.75. For any combination of j and a other than $j = 3$ and $a = 5.25$, the S_{11} values at $f1$ and/or $f2$ are high. Hence, the combination of parameters $j = 3$ and $a = 5.25$ was concluded as most suitable for further studies.

Table 1. Effect of j and a on S_{11}.

Parameter value j	a	$f1$ (GHz)	S_{11} (dB)	$f2$ (GHz)	S_{11} (dB)
2.5	5.25	2.1796	-21.86	6.153	-12.85
3	5.25	2.4523	-24.795	5.6497	-22.99
4	5.25	3.048	-17.473	6.07	-14.85
3	4.75	2.446	-25	6.253	-17.23
3	5.75	2.4545	-22.744	5.16	-13.78

Figure 6 shows the result of S_{11} for constant a and varied j. The values of S_{11} mentioned in Table 1 are obtained from this figure. Figure 7 shows the result of S_{11} for constant j and varied a. The values of S_{11} mentioned in Table 1 are obtained from this figure.

When the designed dual band antenna is integrated with proposed EBG, the above values change to $S_{11} = -24.7955$ dB at frequency of 2.4523 GHz and $S_{11} = -22.9882$ dB at frequency of 5.6497 GHz. Mainly the bandwidth of antenna with EBG exhibits improvement as compared to that with only antenna. Reflection coefficients (simulated & measured) of EBG integrated with antenna are compared in Figure 9. It also shows fabricated antenna integrated with EBG. Measured S_{11} is found to be -20.89 dB at center frequency of 2.44 GHz and -15.9 dB at center frequency of 5.82 GHz. Simulated

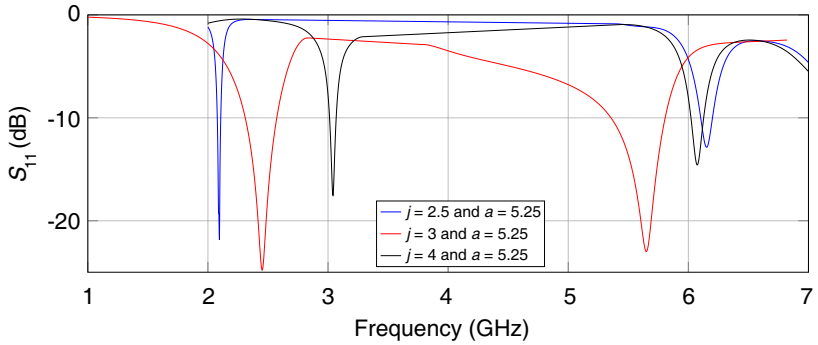

Figure 6. Simulated S_{11} of antenna with EBG with j as parameter.

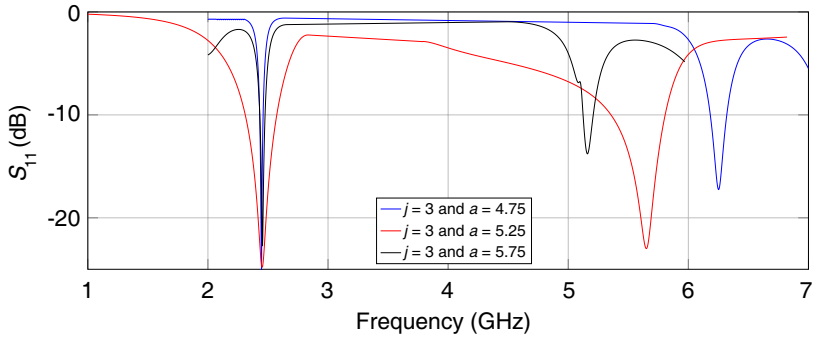

Figure 7. Simulated S_{11} of antenna with EBG with a as parameter.

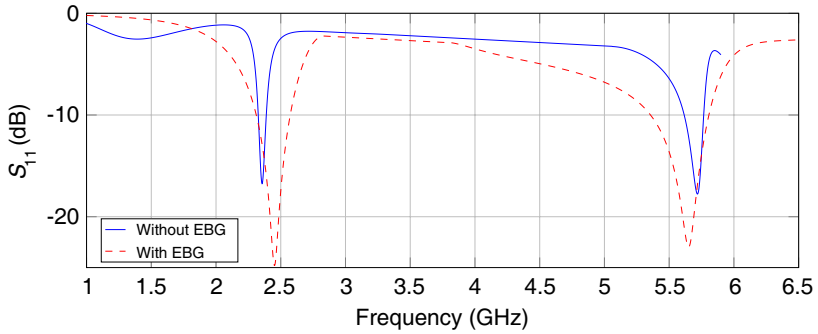

Figure 8. Simulated S_{11} of antenna without and with EBG.

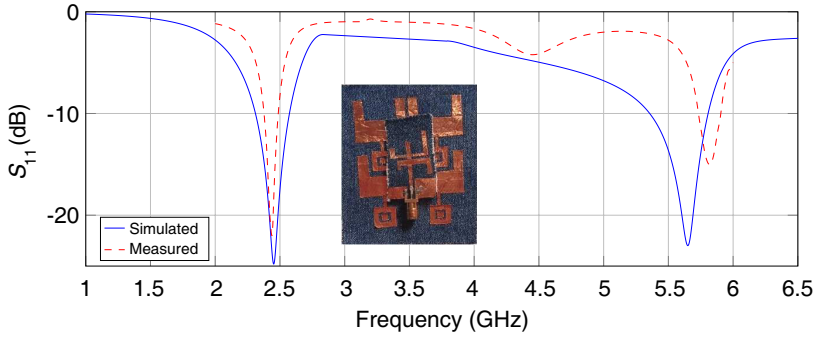

Figure 9. Comparison of reflection coefficient (simulated and measured) in case of antenna with EBG.

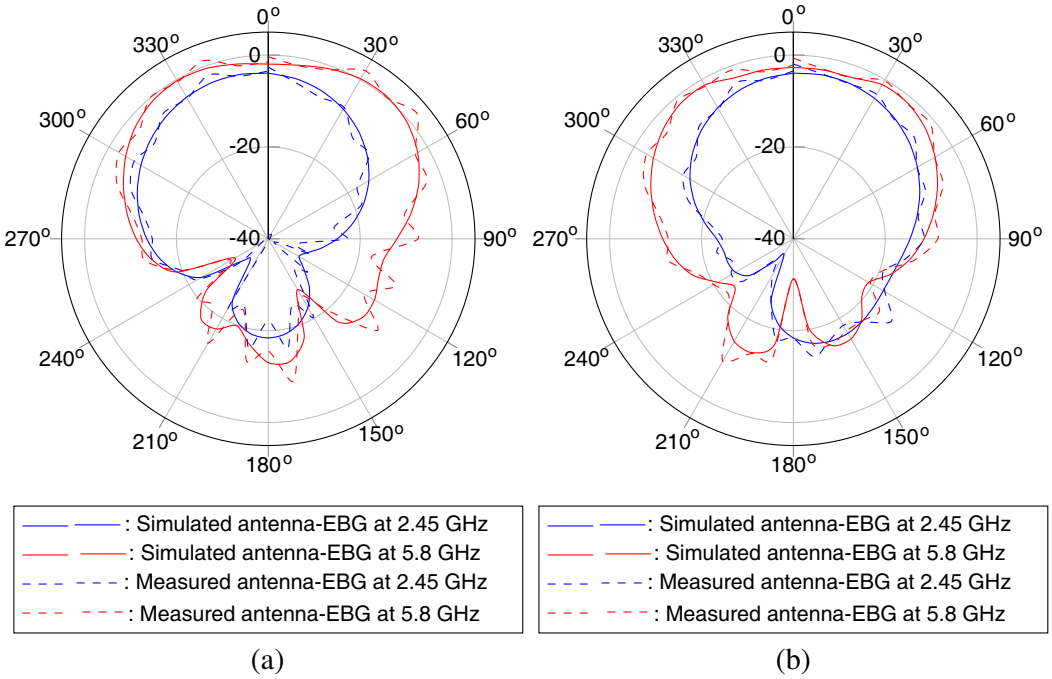

Figure 10. Simulated and measured radiation patterns of antenna with EBG in (a) E plane and (b) H plane.

and measured results are different due to manual fabrication process error and also assembly process followed for antenna with EBG.

Simulated radiation pattern of antenna with EBG in Y-Z plane which is E-plane and in X-Z which is H-plane at frequencies of 2.45 GHz and 5.8 GHz are shown in Figure 10. The E-plane radiation pattern exhibits maximum radiation in Z-direction. However its null is seen in Y-direction at both frequencies. Figure 10 also shows radiation patterns obtained experimentally in both E and H planes at both frequencies. The simulated and measured results are in close agreement.

3.3. Antenna Bending Effect

To see the effect of bending, the fabrication of 3 cylinders made up of foam & of different diameters was carried out. Figure 11 shows fabricated cylinders with proposed antenna mounted. Diameters of cylinder in mm were 80, 100, and 120. These values are close to leg & arm diameters of typical human being. The comparison of measured reflection coefficient antenna with EBG in free space with those

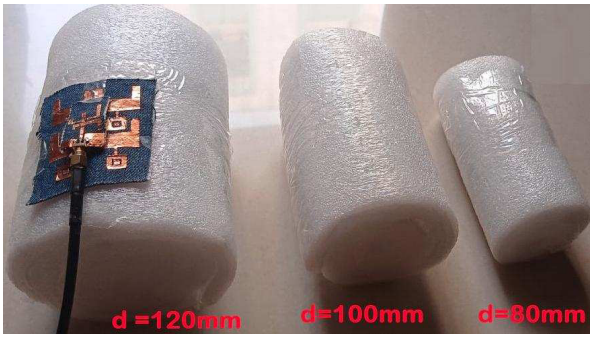

Figure 11. Foam cylinders of various diameters with antenna mounted.

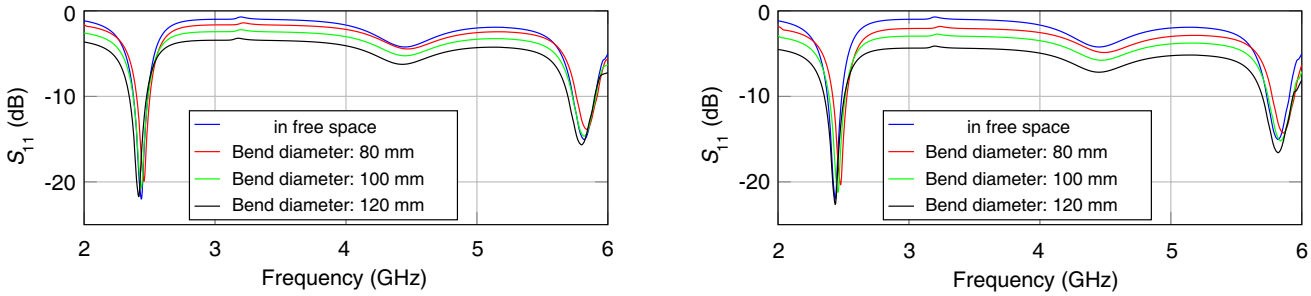

Figure 12. Plot of measured S_{11} of antenna with EBG in free space compared with that for different bending diameters in (a) X and (b) Y direction.

on cylinders of different bending diameters in both X and Y directions was carried out as shown in Figure 12. From Figure 12, is it observed that even though the foam cylinder diameter is altered, the resonance frequency of antenna and its operating frequency band are only slightly shifted. The frequency of operation of antenna is almost preserved. Also, reflection coefficient S_{11} shows a sustained bandwidth under the condition of bending in both x and y directions.

4. PROPOSED EBG AND ANTENNA SAR ANALYSIS

The proposed dual-band EBG structure and antenna have been designed with the intent of obtaining low SAR in wearable applications. Detailed description about SAR, its analysis, etc. could be seen in [22]. SAR analysis was carried out in Ansys HFSS simulation software using a 4-layer body model with properties at 2.45 GHz shown in Table 2. The 4-layer body model has properties at 5.8 GHz as shown in Table 3.

Results of the SAR computed in tissue averaged over 10 g of human body without and with EBG for 2.45 GHz and 5.8 GHz are shown in Figure 13 and Figure 14, respectively. Results of peak SAR values found by simulations are shown in Table 4. The antenna with EBG was experimentally tested in free space and on body for values of S_{11}. Comparison is as shown in Figure 15, and results are found close.

Table 2. Properties of layers in multilayer human model at 2.45 GHz [6].

Layer	Thickness mm	ϵ_r	Conductivity σ (S/m)	Density kg/m^3
Skin	2	37.95	1.49	1001
Fat	5	5.27	0.11	900
Muscle	20	52.67	1.77	1006
Bone	13	18.49	0.82	1008

Table 3. Properties of layers in multilayer human model at 5.8 GHz [23].

Layer	Thickness mm	ϵ_r	Conductivity σ (S/m)	Density kg/m^3
Skin	2	35	3.8	1001
Fat	5	4.95	0.3	900
Muscle	20	48.4	5.12	1006
Bone	13	15.4	2.15	1008

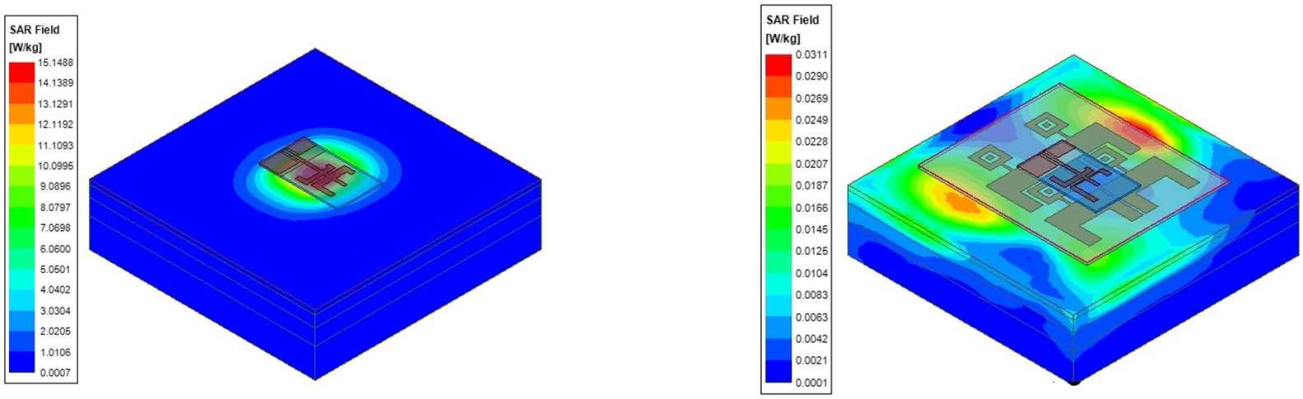

(a) (b)

Figure 13. SAR values in four layer body model without EBG and with EBG at 2.45 GHz by simulations, (a) without EBG, (b) with EBG.

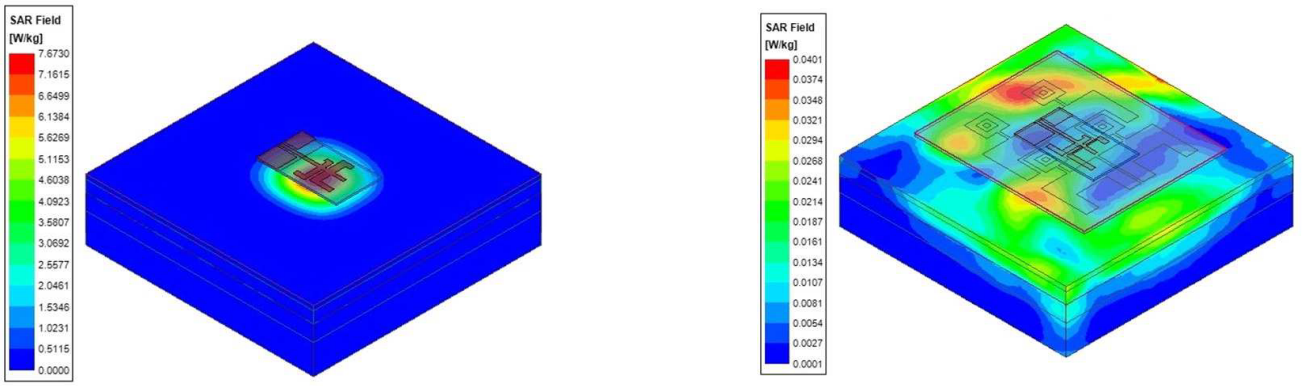

(a) (b)

Figure 14. SAR values in four layer body model without EBG and with EBG at 5.8 GHz by simulations, (a) without EBG, (b) with EBG.

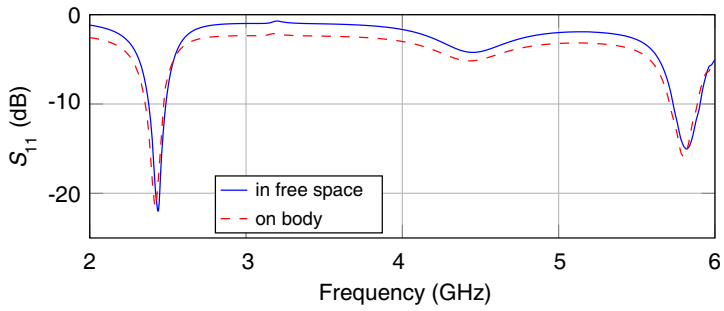

Figure 15. Measured reflection coefficient of antenna with EBG in free space compared with that on body.

The comparison of proposed EBG was carried out with EBG/AMC structures used for similar frequencies and is shown in Table 5. The proposed EBG structure has less number of units than reported EBG/AMC structures. In dual band frequencies considered in this work, the proposed EBG structure has the lowest patch width.

Comparison of proposed EBG was also carried out with reported structures in terms of volume and

Table 4. Simulated SAR values (W/kg) of proposed antenna for 10 g tissue.

Frequency in GHz	Antenna without EBG	Antenna with EBG
2.45	15.14	0.0311
5.8	7.6	0.0401

Table 5. Comparison of proposed EBG with exiting structures in terms of number of units and patch width.

Ref.	No. of EBG unit cells	$f1/f2$ (GHz)	EBG Patch width ($\lambda \times \lambda$)	ϵ_r/h
[9]	3×3	2.45/5	0.327λ	1.38/1.1
[14]	4×4	2.45/5.8	0.22λ	1.2/2
[15]	2×2	2.45/3.4/5.8	0.296λ	1.2/1.1
[16]	3×3	2.4/5.5	0.204λ	1.7/1.6
[17]	3×1	2.4/5.2	0.234λ	1.22/2.5
[18]	2×3	2.45/5.8	0.21λ	1.7/1.6
Proposed	2×2	2.45/5.8	0.192λ	1.7/1

Table 6. Comparison of proposed EBG with existing structures in terms of volume and SAR.

Ref.	Volume mm^3	SAR W/kg (at $f1/f2$) 1 g	SAR W/kg (at $f1/f2$) 10 g
[9]	$120 \times 120 \times 4.3$	0.079/0.127	0.043/0.090
[10]	$100 \times 100 \times 4.5$	-/-	0.0464/0.0300
[14]	$84 \times 84 \times 2$	0.972/2.80	0.668/1.51
[15]	$69 \times 69 \times 5$	-/-	0.47/0.86/0.14
[18]	$42 \times 63 \times 8$	0.34/0.27	-/-
Proposed	$63 \times 75 \times 2.7$	0.0664/0.1067	0.0301/0.0401

effect on SAR and is shown in Table 6. The proposed dual-band EBG has reasonably lower volume and also SAR within acceptable limits.

5. CONCLUSIONS

The design, analysis, simulations, and important experimental measurements on a proposed rectangular embedded dual-band EBG structure have been attempted in this work. The design of dual-band antenna at dual frequencies 2.45 GHz and 5.8 GHz has been carried out with the aid of HFSS and further integrated with the proposed EBG structure. Important experimental measurements on antenna with and without EBG have been done and found close to designed values. Measured S_{11} exhibits that the designed antenna with EBG has good impedance matching at both the frequencies in the ISM band. Also, the proposed EBG with antenna has smaller volume than those already reported. The analysis of bending and on-body measurements have been attempted, and results are found to be stable. The antenna has been placed on a four layer body model, and subsequently simulation studies have been carried out in the absence and presence of EBG structure. The SAR in simulated human body model with proposed EBG structure is acceptable as per international standards. Hence, the proposed dual-band EBG structure forms a suitable candidate for wearable applications.

REFERENCES

1. Zhang, K., P. J. Soh, and S. Yan, "Design of a compact dual-band textile antenna based on metasurface," *IEEE Transactions on Biomedical Circuits and Systems*, Vol. 16, No. 2, 211–221, 2022, doi: 10.1109/TBCAS.2022.3151243.
2. Bhattacharjee, S., S. Maity, S. R. B. Chaudhuri, and M. Mitra, "A compact dual-band dual-polarized omnidirectional antenna for on-body applications," *IEEE Transactions on Antennas and Propagation*, Vol. 67, No. 8, 5044–5053, Aug. 2019, doi: 10.1109/TAP.2019.2891633.
3. Joshi, R., E. F. N. Mohd Hussin, P. J. Soh, Mohd F. Jamlos, H. Lago, A. A. Al-Hadi, and S. K. Podilchak, "Dual-band, dual-sense textile antenna with AMC backing for localization using GPS and WBAN/WLAN," *IEEE Access*, Vol. 8, 89468–89478, 2020, doi: 10.1109/ACCESS.2020.2993371.
4. El Atrash, M., M. A. Abdalla, and H. M. Elhennawy, "A wearable dual-band low profile high gain low SAR antenna AMC-backed for WBAN applications," *IEEE Transactions on Antennas and Propagation*, Vol. 67, No. 10, 6378–6388, Oct. 2019, doi: 10.1109/TAP.2019.2923058.
5. Velan, S., S. E. Florence, K. Malathi, S. Aswathy, R. Chinnambeti, S. Ramprabhu, and P. J. Kizhekke, "Dual-band EBG integrated monopole antenna deploying fractal geometry for wearable applications," *IEEE Antennas Wireless Propag. Lett.*, Vol. 14, 249–252, 2015.
6. Ashyap, A. Y. I., Z. Z. Abidin, S. H. Dahlan, H. Majid, S. M. Shah, M. R. Kamarudin, and A. Alomainy, "Compact and low-profile textile EBG-based antenna for wearable medical applications," *IEEE Antennas and Propagation Magazine*, Vol. 16, No. 1, 2550–2553, 2017.
7. Guido, K. and A. Kiourti, "Wireless wearables and implants: A dosimetry review," *Bioelectromagnetics*, Vol. 41, 3–20, 2020.
8. Ashyap, A. Y. I., S. H. B. Dahlan, Z. Z. Abidin, M. I. Abbasi, K. R. Kamarudin, H. A. Majid, M. H. Dahri, M. H. Jamaluddin, and A. Alomainy, "An overview of electromagnetic band-gap integrated wearable antennas," *IEEE Access*, Vol. 8, 7641–7658, Jan. 2020, doi: 10.1109/ACCESS.2020.2963997.
9. Zhu, S. and R. Langley, "Dual-band wearable textile antenna on an EBG substrate," *IEEE Transactions on Antennas and Propagation*, Vol. 57, No. 4, 926–935, Apr. 2009.
10. Yan, S., P. J. Soh, and G. A. E. Vandenbosch, "Low profile dual band textile antenna with artificial magnetic conductor plane," *IEEE Transactions on Antennas and Propagation*, Vol. 61, No. 12, 6487–6490, Dec. 2014.
11. Yan, S., P. J. Soh, and G. A. E. Vandenbosch, "Compact all-textile dualband antenna loaded with metamaterial inspired structure," *IEEE Antennas Wireless Propag. Lett.*, Vol. 14, 1486–1489, 2014.
12. Qiang, B. and R. J. Langley, "Crumpled integrated AMC antenna," *Electronics Letters*, Vol. 45, 662–663, 2009, doi: 10.1049/el.2009.0864.
13. Gao, G.-P., B. Hu, S.-F. Wang, and C. Yang, "Wearable circular ring slot antenna with EBG structure for wireless body area network," *IEEE Antennas Wireless Propag. Lett.*, Vol. 17, No. 3, 434–437, Mar. 2018.
14. Gao, G., B. Hu, S. Wang, and C. Yang, "Wearable planar inverted-F antenna with stable characteristic and low specific absorption rate," *Microwave and Optical Technology Letters*, Vol. 60, No. 4, 876–882, Apr. 2018.
15. El May, W., I. Sfar, J. M. Ribero, and L. Osman, "Design of low-profile and safe low SAR tri-band textile EBG-based antenna for IoT applications," *Progress In Electromagnetics Research Letters*, Vol. 98, 85–94, 2021.
16. Mantash, M., A. C. Tarot, S. Collardey, and K. Mahdjoubi, "Design methodology for wearable antenna on artificial magnetic conductor using stretch conductive fabric," *Electronics Letters*, Vol. 52, 95–96, 2016.
17. Afridi, A., S. Ullah, S. Khan, A. Ahmed, A. H. Khalil, and M. A. Tarar, "Design of dual band wearable antenna using metamaterials," *Journal of Microwave Power and Electromagnetic Energy*, Vol. 47, 126–137, 2013.

18. Mersani, A., O. Lotfi, and J.-M. Ribero, "Design of a textile antenna with artificial magnetic conductor for wearable applications," *Microwave and Optical Technology Letters*, Vol. 60, 1343–1349, 2018, 10.1002/mop.31158.
19. Dalal, P. and S. K. Dhull, "Eight-shaped polarization-dependent electromagnetic bandgap structure and its application as polarization reflector," *International Journal of Microwave and Wireless Technologies*, 1–9, 2021, doi: 10.1017/S1759078721000271.
20. Yang, F. and Y. Rahmat Samii, *Electromagnetic Band Gap Structures in Antenna Engineering (The Cambridge RF and Microwave Engineering Series)*, Cambridge University Press, Cambridge, 2008, doi: 10.1017/CBO9780511754531.
21. Keshwani, V. R., P. P. Bhavarthe, and S. S. Rathod, "Eight shape electromagnetic band gap structure for bandwidth improvement of wearable antenna," *Progress In Electromagnetics Research C*, Vol. 116, 37–49, 2021.
22. Keshwani, V. R. and S. S. Rathod, "Assessment of SAR reduction in wearable textile antenna," *2021 International Conference on Communication Information and Computing Technology (ICCICT)*, 1–5, 2021, doi: 10.1109/ICCICT50803.2021.9510174.
23. Gabriel, C., "Compilation of the dielectric properties of body tissues at RF and microwave frequencies," *Report N.AL/OE-TR-1996-0037, Occupational and Environmental Health Directorate*, Radiofrequency Radiation Division, Brooks Air Force Base, Texas, USA, 1996.